Perspective

Thermal Ablation Therapy for Focal Malignancy: A Unified Approach to Underlying Principles, Techniques, and Diagnostic Imaging Guidance

S. Nahum Goldberg [1], G. Scott Gazelle [2], Peter R. Mueller [2]

Percutaneous imaging-guided ablative therapies using thermal energy sources such as radiofrequency (RF), microwave, laser, and high-intensity focused sonography have received much recent attention as minimally invasive strategies for the treatment of focal malignant diseases [1, 2]. Possible advantages of ablative therapies compared with surgical resection include the anticipated reduction in morbidity and mortality, low cost, suitability for real-time imaging guidance, and the ability to perform ablative procedures on outpatients. Promising results have been reported in early clinical trials for the treatment of hepatocellular carcinoma [3–6], hepatic [7–11] and cerebral [12, 13] metastases, renal [14] and retroperitoneal [15] tumors, and bony lesions, including osteoid osteomas [16, 17].

Many similarities exist among the thermal methods of ablation. However, the individual techniques used for destruction are often discussed only within the framework of that particular technology (RF, laser, and so forth), rather than from a global perspective of looking at thermal therapy as a whole. This outlook may be shortsighted because many aspects of thermal ablation have been independently rediscovered. For example, innovations to increase energy deposition, such as reducing excess heat near the thermal source by internal cooling, have been shown useful for many techniques including RF, laser, high-intensity sonography, and microwave [18–21]. Additionally, the biophysical limitations that prevent adequate tumor ablation are innate to tumor biology and will pose similar problems for all thermal ablation methods. A key example is the effect of tissue blood flow that limits coagulation in vivo [22–25]. Furthermore, issues related to monitoring of ongoing ablation procedures apply equally to all these methods, and imaging findings are remarkably similar at follow-up.

Therefore, this perspective proposes a unified framework for discussing the various aspects of all thermal ablation therapies as they relate to the treatment of focal malignancies. This framework is based loosely on Pennes' [26] bioheat equation, which takes into account the factors that influence tissue heating (Appendix 1). Briefly, the extent of coagulation necrosis induced in a given lesion is equal to the energy deposited, modified by local tissue interactions, minus the heat lost before inducing thermal damage.

Induction of Coagulation Necrosis

The main aim of thermal tumor ablation therapy is to destroy an entire tumor by using heat to kill the malignant cells in a minimally invasive fashion without damaging adjacent vital structures. This therapy often includes the treatment of a 0.5- to 1-cm margin of apparently healthy tissue adjacent to the lesion to eliminate microscopic foci of disease and the uncertainty that often exists regarding the precise location of actual tumor margins. However, tumor cells can be effectively destroyed by cytotoxic heat from different sources. As long as adequate heat can be generated throughout the tumor, our objective of eradicating the tumor will be accomplished. Therefore, it is necessary to understand how heat interacts with tissue to induce cell death.

Cellular homeostasis can be maintained with mild elevation of temperature to approximately 40°C. When temperatures are increased to 42–45°C (hyperthermia), cells become more susceptible to damage by other agents such as chemotherapy and radiation [27, 28]. However, even prolonged heating at these temperatures will not kill all cells in a given volume because continued cellular functioning and tumor growth can be observed after relatively long exposure to these temperatures. When temperatures are increased to 46°C for 60 min, irreversible cellular damage occurs [29]. Increasing the temperature only several degrees to 50–52°C markedly shortens the time necessary

Received April 26,1999; accepted after revision July 19, 1999.

[1] Department of Radiology, Beth Israel Deaconess Medical Center, 330 Brookline Ave., Boston, MA 02215. Address correspondence to S. N. Goldberg.

[2] Department of Radiology, Massachusetts General Hospital, 32 Fruit St., Boston, MA 02114.

AJR 2000;174:323–331 0361–803X/00/1742–323

to induce cytotoxicity (4–6 min) [30]. Between 60° and 100°C, near instantaneous induction of protein coagulation that irreversibly damages key cytosolic and mitochondrial enzymes and nucleic acid–histone complexes occurs [31, 32]. Cells experiencing this extent of thermal damage most often, but not always, undergo coagulative necrosis over the course of several days. The term "coagulation necrosis" has been used to denote irreversible thermal damage to cells, even if the ultimate manifestations of cell death do not fulfill the strict histologic criteria of coagulative necrosis. Temperatures greater than 105°C result in tissue boiling, vaporization, and carbonization. These processes usually retard optimal ablation because of a resultant decrease in energy transmission [30]. Thus, a key aim for ablative therapies is achieving and maintaining a 50–100°C temperature range throughout the entire target volume.

Sources of Thermal Energy

Multiple energy sources have been used to provide the heat necessary to induce coagulation necrosis. Electromagnetic energy has been used in the form of both RF and microwaves [33, 34]. Photocoagulation uses intense pulses of light produced by a laser as the energy source [35]. High-intensity focused sonography uses sound energy to produce heat [36, 37]. Injection of heated fluids, including saline, ethanol, and contrast material, has been used to induce coagulation by direct thermal contact [38].

For most methods of thermal ablation, energy is applied percutaneously with needle-shaped applicators. These high doses of energy usually concentrate around the applicator and require heat conduction through the tissue from this local thermal reservoir to coagulate deeper tissues. For RF, radio waves emanate from the noninsulated distal portion of the electrode. Heat is produced by resistive forces (i.e., ionic agitation) surrounding the electrode as the radio waves attempt to find their ground, usually a foil pad attached to the patient's back or thighs. For microwave, needle-shaped electrodes function as an antenna that concentrates energy around the applicator and heats the tissue by friction, as polar molecules attempt to align with the electromagnetic field. For photocoagulation, thin optical fibers that conduct laser energy are placed through needles positioned in the tumor. These bare fibers transmit the intense light into the tissue, where the light is converted to heat. For both microwave and laser, the depth of energy penetration can be altered by altering the frequency of the energy source. Percutaneous probes containing multiple small piezoelectric transducers can deposit sufficient sound energy to heat adjacent tissues. Another potential application of sonographic energy has been incorporated into extracorporeal systems of energy delivery. These systems rely on focusing intense energy from an external sonographic source. Unfortunately, the maximum size for a single ablative focus has thus far approximated a grain of rice; therefore, complex imaging-guided systems are necessary to adequately treat larger areas [36]. However, improvements in technology may ultimately allow the treatment of larger foci.

Heat–Tissue Interactions

To adequately destroy a tumor, the entire lesion must be subject to cytotoxic temperatures. However, multiple and often tissue-specific limitations that prevent heating of the entire tumor volume exist. Most important, heterogeneity of heat deposition occurs throughout a given lesion to be treated. For all percutaneous methods, heat deposition is greatest surrounding the probe, with less heat deposited deeper in the tissues (Fig. 1). This concentration of heat is caused by both a rapid falloff of energy from the applicator and poor heat conduction in the tissues. Additionally, the total quantity of energy that can be deposited in the tissues is limited by tissue boiling and vaporization at extreme temperatures (>105°C). When tissue vaporization occurs, gas is formed. For all methods, this gas serves as an insulator that prevents heat spread. For RF, gas formation increases tissue impedance that prevents deposition of the heating current. Energy deposition with a single applicator (i.e., a monopolar RF electrode or a single laser fiber) produces coagulation measuring only up to 1.6 cm in diameter [39–41].

Several strategies have been developed to improve tissue–energy interactions for thermal ablation therapy, with the goal of increasing the region of induced coagulation to enable the treatment of most clinically relevant tumors (i.e., those measuring >1–2 cm in diameter) (Table 1). These strategies can be classified as those that permit an increase in overall energy (amount and rate) deposited, those that improve heat conduction within the tissue, and those that decrease tumor tolerance to heat.

Increasing Energy Deposition

A common method for increasing energy deposition throughout an entire lesion has been to repeatedly insert multiple RF, laser, and microwave probes into the tissue to increase the diameter of induced coagulation [3, 5, 7, 36]. This approach is both time-consuming and difficult to use in the clinical setting, particularly because multiple overlapping treatments must be

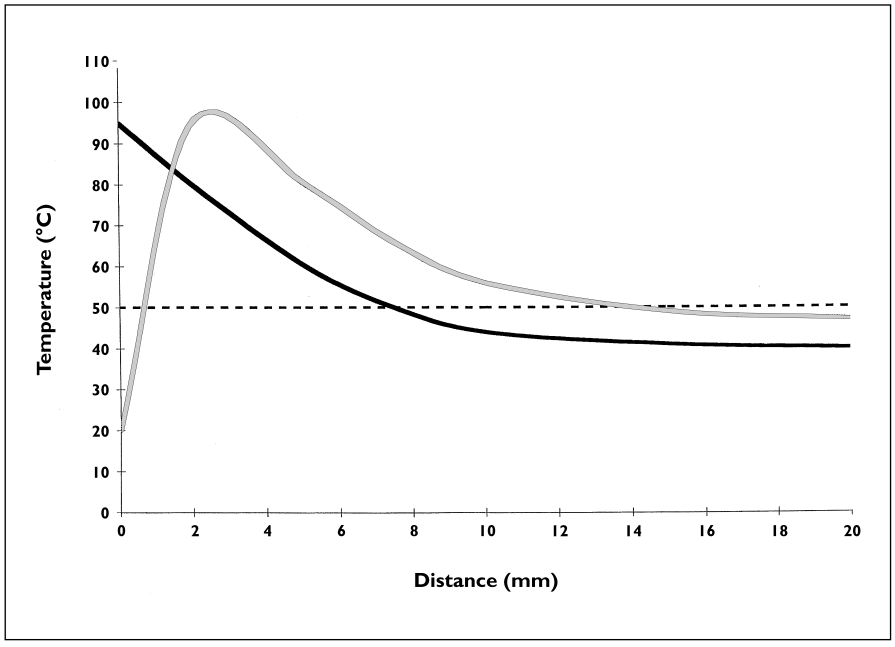

Fig. 1.—Graph shows tissue temperature profile for thermal ablation with and without cooling of energy applicator. Temperatures were generated by applying radiofrequency (RF) for 12 min at maximum tissue temperature of 95°C to in vivo swine muscle (methodology adapted from [19]). Internal cooling permits greater energy deposition in tissues resulting in greater heating at distance from electrode. This cooling strategy has been used successfully for multiple energy sources. Solid black line represents conventional (RF), solid gray line is cooling, and broken line is coagulation threshold.

TABLE 1 Coagulation Necrosis Produced by Thermal Ablation

Method	Energy Source	Coagulation Ex Vivo	Coagulation in Tumors (cm)[a]	Remarks
Single applicator	RF, ILP, MW, US	1.6 cm	0.8–1.6	
Multiprobe arrays	RF, ILP, MW	4.0 cm	3.0–5.0	Technical limitations
Hooked array[b]	RF	4.0 cm	2.0–4.0	Multiple applications
Saline infusion	RF	4.1 cm	1.2–3.9	Irregular shape
Internally cooled applicator	ILP, RF, US, MW	4.5 cm	1.8–3.6	
Pulsed energy	ILP, RF	4.5 cm	2.8–4.2	
Cluster electrodes	RF	6.5 cm	4.2–7.0	
Focused extracorporeal	HIFU[c]	1 × 2 mm	< 2	Advanced targeting

Note.—Data compiled from [1, 2]. RF = radiofrequency, ILP = interstitial laser photocoagulation, MW = microwave, US = percutaneous ultrasound probes, HIFU = high-intensity focused ultrasound.

[a] Represents maximum achieved using specified technique. Results reported for liver tumors were achieved with optimal parameters.

[b] RF has most often been applied multiple times in a single session.

[c] Advanced targeting strategies are required to obtain larger contiguous areas of coagulation.

performed in a contiguous fashion (in all three dimensions) to destroy the entire lesion. Simultaneous application of energy using arrays can reduce the duration of therapy [42, 43]. However, the precise positioning of multiple probes can be technically challenging. The development of umbrella RF electrodes with multiple hooked arrays has overcome some of these problems and has enabled the creation of larger zones of coagulation [3, 9, 44].

Much recent development has centered on strategies that preferentially cool tissues nearest the probe in an attempt to increase overall energy deposition. Internally cooled electrodes have been used with RF, microwave, high-intensity sonography, and laser [18–21]. For internally cooled devices, two internal lumens permit the delivery of chilled perfusate to the tip of the electrode and allow the warmed effluent to be removed to a collection unit outside the body. This procedure causes a heat-sink effect that removes heat closest to the electrode (Fig. 1). Pulsing of energy is another strategy that has been used with RF and laser to increase the mean intensity of energy deposited. When pulsing is used, periods of high energy deposition are rapidly alternated with periods of low energy deposition. If a proper balance between high and low energy deposition is achieved, preferential tissue cooling occurs adjacent to the applicator during periods of minimal energy deposition without significantly decreasing heating deeper in the tissue. Thus, even greater energy can be applied during periods of high energy deposition, enabling deeper heat penetration and greater tissue coagulation [45, 46]. Combination of both internal cooling and pulsing has been shown as synergistic with even greater tissue destruction observed than with either method alone [47].

Improved Tissue Heat Conduction

Improved heat conduction within the tissues by injection of saline and other compounds has also been proposed [48–50]. The heated liquid spreads thermal energy farther and faster than heat conduction in healthy "solid" tissue. An additional potential benefit of simultaneous saline injection is that it increases tissue ionicity, thereby enabling greater current flow. Similarly, amplification of current shifts with iron compounds injected or deposited in the tissues before ablation has been used for RF and microwave [50].

Another primary factor that can alter the extent of coagulation necrosis is tissue composition because heat conducts through different tissues at various rates [4, 51]. For example, poor thermal conduction has been documented for bone compared with muscle [51]. This fact has been an advantage in the treatment of hepatocellular carcinomas and vertebral body lesions. Livraghi et al. [4] have described the "oven effect" in which cirrhotic tissue insulates hepatocellular carcinoma nodules and increases temperatures within the targeted tumor during RF therapy. Dupuy et al. [51] have shown that cortical bone also serves as an insulator, enabling treatment of vertebral body lesions without damaging the spinal cord.

Strategies That Decrease Tumor Tolerance to Heat

Strategies that decrease tumor tolerance to heat have been proposed but are not yet well studied. Theoretically, previous insult to the tumor cells by cellular hypoxia caused by vascular occlusion or antiangiogenesis-factor therapy (i.e., endostatin) or prior tumor cell damage from chemotherapy or radiation could be used to increase tumor sensitivity to heat. Synergy between chemotherapeutic agents and hyperthermic temperatures (42–45°C) has already been established [27, 28].

Sources of Heat Loss

Biophysical aspects of tumor–heat interaction must be taken into account when performing thermal ablation therapies. The extent of induced coagulation compared with the reproducible results obtainable in ex vivo tissue is more limited and variable in vivo and in tumors. Substantial evidence suggests that perfusion-mediated tissue cooling (vascular flow) reduces the extent of coagulation necrosis produced by thermal ablation [22–25]. Decreased volume of coagulation has been observed when comparing in vivo liver with ex vivo and nonperfused liver, with coagulation necrosis in vivo often shaped by hepatic vasculature. Furthermore, experiments altering hepatic perfusion by vascular occlusion during RF and laser ablation of healthy liver and tumors strongly support the contention that perfusion-mediated tissue cooling is largely responsible for reduction in observed coagulation [22–25]. A close correlation between the diameter of RF-induced coagulation and pharmacologically modulated blood flow in the healthy liver has also been shown [23]. Thus, with in vivo tissues a heat-sink effect prevents achieving the cytotoxic temperature necessary to induce coagulation (50–60°C) in highly vascular regions of a tumor (i.e., the peripheral tumor–parenchyma interface).

On the basis of these observations, several strategies for reducing blood flow during ablation therapy were proposed. Total portal inflow occlusion (Pringle's maneuver) has been used but requires open laparotomy [22]. Angiographic balloon occlusion can be used but may not prove adequate for intrahepatic ablation because of the dual hepatic blood supply with redirection of compensated flow [22]. Embolotherapy before ablation with particulates that occlude sinusoids such as a gelatin sponge (Gelfoam; Upjohn, Kalamazoo, MI) or iodized oil (Lipiodol; Roissey-Charles-de-Gaullle, France) may overcome this limitation [52]. Pharmacologic

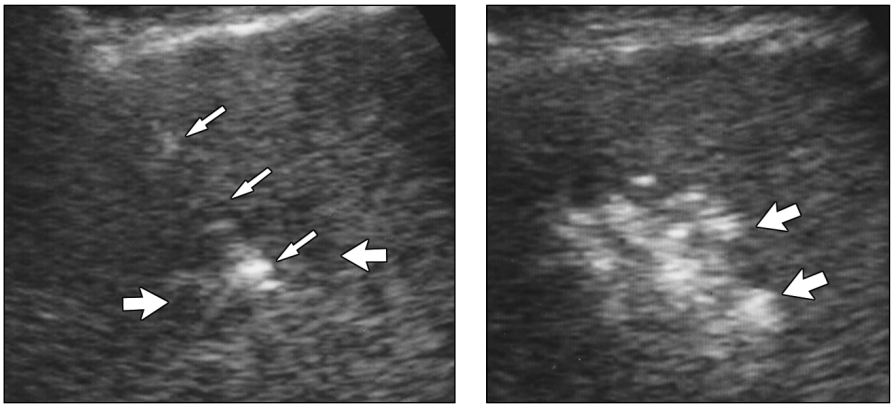

A B

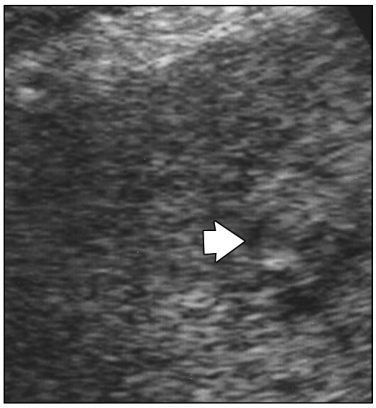

C

Fig. 2.—63-year-old man with 2.4-cm colorectal metastasis undergoing sonographically guided radiofrequency (RF) ablation.
A, Gray-scale sonogram shows metastasis (*large arrows*) before RF treatment. Electrode (*small arrows*) has been percutaneously inserted into tumor.
B, Sonogram obtained during RF application shows progressive echogenicity surrounding tip of electrode (*arrows*).
C, Sonogram obtained 15 min after RF ablation shows no echogenicity within tumor (*arrow*).

modulation of blood flow and antiangiogenesis therapy are theoretically possible but should currently be considered experimental.

Diagnostic Imaging for Thermal Ablation Therapy

Diagnostic imaging applications can accomplish three distinct tasks for thermal ablation procedures. These tasks include targeting of the lesion to be treated (i.e., ensuring optimal positioning of the energy applicator during ablation), guidance for energy deposition for the duration of the treatment plan, and assessment of results at follow-up. The imaging appearances for laser, microwave, and RF are remarkably similar for any given organ and degree of tissue heating. Needlelike applicators will all look approximately the same for any given technique, and coagulated (or heated) tissues should theoretically appear identical for a given extent of coagulation, regardless of how it is induced.

Diagnostic Imaging for Lesion Targeting

Multiple imaging techniques (sonography, CT, and MR imaging) can be used to guide the percutaneous placement of thermal energy applicators into the selected target [1, 2]. Because in most cases adequate lesion conspicuity and visualization of the applicator can be achieved with any of these methods, the choice of imaging technique is often dictated by personal preference or research interests. Most imaging-guided thermal ablation procedures have thus far been performed with sonography (Fig. 2). Benefits claimed for sonography include the real-time visualization of applicator placement, portability of the technology, nearly universal availability, low cost, and ability to target and guide ablation therapy with intracavitary endoluminal transducers (i.e., for transrectal or transgastric energy application to the prostate and abdominal organs). Limitations of sonography include occasional poor lesion visualization as a result of a lack of innate tissue conspicuity or overlying bone- or gas-containing structures. MR imaging generally provides greatest tumor-to-tissue conspicuity and the ability to use multiplanar guidance. However, this technology is relatively expensive, requires specialized ablation equipment that is compatible with a high magnetic field, and is the least available for general clinical use. CT and, more recently, real-time CT fluoroscopy have also been used to ensure adequate positioning of the energy applicator. Though CT fluoroscopy has not been extensively evaluated, it is fair to say that CT falls between sonography and MR imaging with respect to cost, tissue contrast, and complexity. In our clinical practice, we use a combined approach of CT fluoroscopy and sonography at the same setting to document optimal RF electrode positioning (Fig. 3B).

Diagnostic Imaging to Guide Therapy

To prevent under- or overtreatment of a lesion, it is essential to have accurate and reliable methods for determining the adequacy of therapy. Thus, significant investigation into the development of imaging strategies that enable rapid assessment of the extent of tissue destruction induced by thermal ablation is being conducted. Despite initial enthusiasm, gray-scale sonographic findings observed during the thermal ablation procedure are not sufficiently accurate in predicting the extent of coagulation [7, 8, 53]. The progressively increasing hyperechogenic focus often seen surrounding the distal portion of the applicator during the application of energy represents microbubbles of gas that form in the heated tissue and does not represent tissue coagulation [54] (Fig. 2B). This hyperechogenic region can be variable in size, may be quite irregular in shape and contour, and often shows complete resolution within 1 hr of ablation (Fig. 2C). Additionally, this intense echogenicity can often obscure the energy applicator and tumor while increasing the difficulty of repositioning for further treatment.

Conventional color-flow and power Doppler sonography have similarly not been found useful in assessing the extent of induced coagulation [7, 8]. However, in one study contrast-enhanced color Doppler sonography with a synthetic microbubble sonographic contrast agent was able to achieve 92% accuracy in predicting the extent of coagulation in VX2 rabbit tumors immediately after RF ablation [55]. Additionally, sonographic contrast material has been used to direct a second energy application to residual enhancing (and presumably viable) foci within the treatment zone [56].

For solid organs such as the liver, unenhanced CT scans obtained immediately after ablation often reveal increased density at the center of the treatment zone, most often surrounded by a region of hypoattenuation [3–13, 53, 57, 58]. With the exception of encapsulated lesions such as those of hepatocellular carcinoma, the margins of this outer hypodense

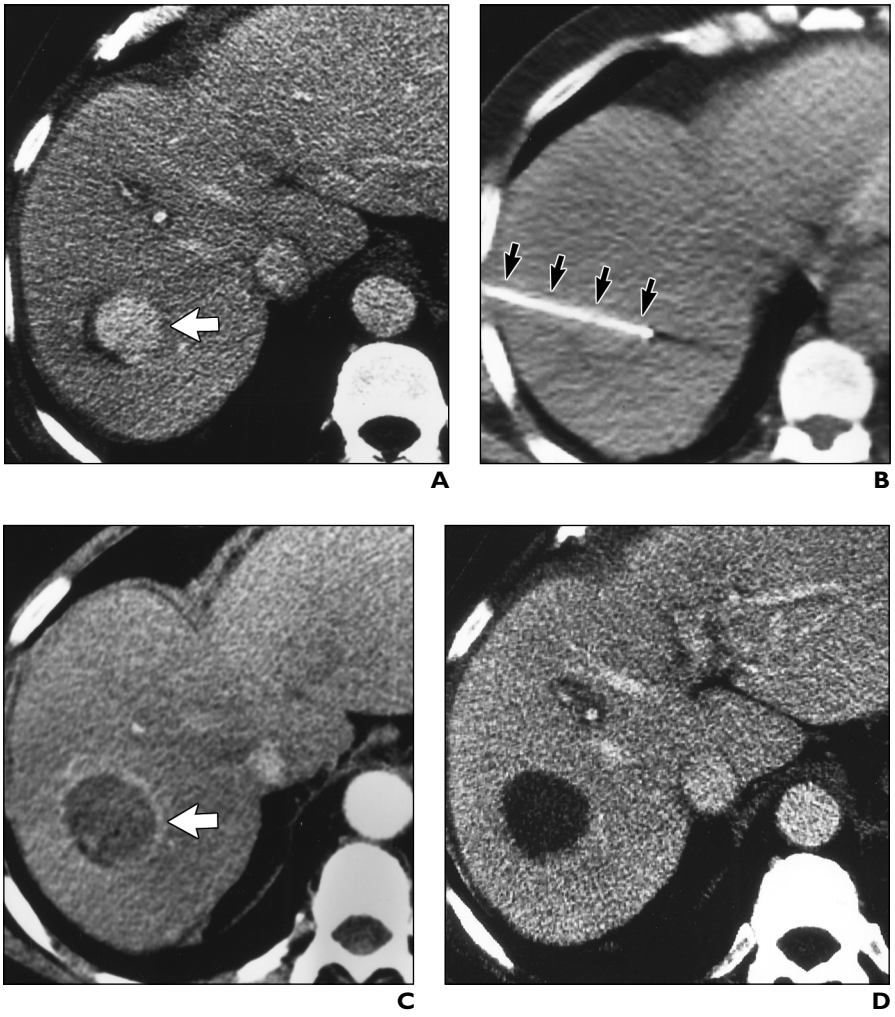

Fig. 3.—58-year-old man with cirrhosis and 4-cm hepatoma treated with radiofrequency (RF) ablation using CT fluoroscopic guidance.
A, Arterial phase CT scan shows hypervascular hepatoma (*arrow*) before RF treatment.
B, CT fluoroscopy image obtained during electrode insertion (*arrows*) shows electrode centered in tumor.
C, Contrast-enhanced CT scan obtained 15 min after procedure shows that entire tumor is devoid of parenchymal enhancement. Enhancing hyperdense rim surrounds treatment zone (*arrow*).
D, Contrast-enhanced CT scan at 6-month follow-up shows no evidence of enhancement or hypervascular rim. These findings suggest, but are not definitive of, adequate treatment.

zone are often too diffuse to be of sufficient sensitivity to assess therapy. However, contrast-enhanced CT is useful in discriminating between ablated and residual viable tumor immediately after thermal ablation because it shows regions of hypoattenuation devoid of characteristic tumorous or parenchymal enhancement in treated portions of the tumor. For intrahepatic metastases, the differentiation of coagulation necrosis from hypoattenuating tumor is usually easiest on images in the equilibrium phase of contrast enhancement (5–10 min after iodinated contrast administration). At this phase, persistent hypoattenuation is seen in coagulated tissues but not in viable tumor [31]. Hepatic arterial phase images are most useful for early-enhancing hepatocellular carcinomas (Fig. 3). Imaging during the hepatic arterial phase can also show a thin rim of contrast material corresponding on histopathology to an early inflammatory reaction to the thermal damage (Fig. 3C). This inflammatory rim can be seen immediately after ablation and often regresses during the first month after treatment.

MR images characteristically reveal altered signal on both T1- and T2-weighted images [53, 57, 59] (Fig. 4). Treated areas are devoid of gadolinium enhancement. Several studies have documented the particular usefulness of decreased signal on T2-weighted images as a marker for induced coagulation [59, 60]. Radiologic–pathologic correlation in both experimental and clinical studies has shown that CT and MR imaging findings predict the region of coagulation to within 2–3 mm [31].

One key advantage of MR imaging over other diagnostic imaging techniques is its ability to aid in determining the extent of coagulation during energy application. Heat-sensitive sequences have been constructed and permit tailoring of energy deposition [61–63]. Such a strategy is most useful in allowing the operator to limit energy deposition when heating adjacent to a critical structure (i.e., nerves) reaches cytotoxic temperatures. Pulsing switches were developed to overcome interference of RF and microwave usage during the acquisition of MR–RF encoded data [64].

Long-Term Imaging Follow-Up

Although initial imaging can serve as a good indication of the adequacy of therapy, the resolution and accuracy of current imaging techniques preclude identification of residual microscopic foci of malignancy, particularly at the periphery of a treated lesion (where blood flow is greatest). These viable tumor foci will inevitably continue to grow and, if untreated, will result in failed therapy. Additionally, considering issues of sampling error and the possible difficulty in differentiating between adequately treated and viable tumors with histopathologic techniques alone, we have not found the use of needle biopsy helpful. Thus, long-term imaging follow-up is necessary to find untreated regions of the tumor or to document complete treatment of a given focal malignancy.

Long-term follow-up of thermal ablation with sonography has limited value [7, 8]. Obscuration of the characteristic peritumoral halo observed before treatment is often seen, and the variability of gray-scale sonographic changes precludes accurate assessment of induced coagulation. Sonographic microbubble blood pool agents such as SH 508 A (Levovist; Schering, Berlin, Germany) may be helpful in differentiating treated tumor from the avascular coagulation at 6 months of follow-up [65].

Contrast-enhanced CT has been the mainstay of long-term imaging follow-up (Figs. 3 and 5). Coagulated nonenhancing regions increase in conspicuity and develop sharper margins by 2 weeks after ablation [31, 53]. Imaging at 6–12 months can show marked regression of the lesion and the region of induced coagulation necrosis. Most commonly, the nonenhancing treatment focus shrinks less than 20% in volume. A peripheral rim that densely enhances on delayed contrast images often surrounds the

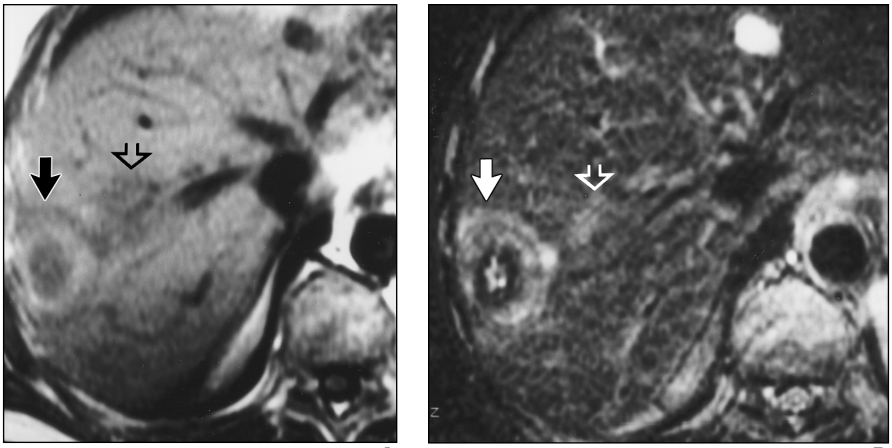

Fig. 4.—74-year-old-man with biopsy-proven colorectal metastasis 3 weeks after radiofrequency ablation of one lesion.
A, T1-weighted image shows heterogeneous but concentric signal throughout treatment zone (*solid arrow*). Second untreated lesion shows traditional signal characteristics (*open arrow*).
B, T2-weighted image shows similar concentric pattern of altered signal in treatment zone (*solid arrow*). Open arrow indicates untreated lesion.
C, Gadolinium-enhanced T1-weighted image shows no evidence of central enhancement. Thin peripheral rim of contrast enhancement is identified (*solid arrow*) and corresponds to early inflammatory response to treatment. Open arrow indicates untreated lesion.

region of coagulation. This finding should not be misconstrued as residual tumor, for experimental and clinical studies have shown this rim to represent an inflammatory reaction to the thermally damaged cells [53, 66]. A bulky irregular rim at the edge of a treatment site is the most common appearance of an incompletely treated lesion (Fig. 6).

When using MR imaging for long-term follow-up (>3 months), we have relied primarily on the presence or absence of gadolinium enhancement in the treated region [8, 53]. In comparison with MR images obtained within 3 days of ablation, we have observed heterogeneous alteration on unenhanced T1- and T2-weighted images (Fig. 4). This changing variability in signal intensity throughout the ablated region is most likely caused by an uneven evolution of the necrotic area and the host response to thermal damage. Hence, these images have been thus far too variable to be relied on as adequate proof of tumor destruction. The multiplicity of potential imaging sequences and parameters used for MR imaging has only further compounded this problem. Further research may ultimately lead to greater insight into the biologic mechanisms that account for such signal heterogeneity. For gadolinium-enhanced images, it is also common to detect a thin rim of enhancement after treatment. As for CT scans, only when this rim appears bulky is this finding to be interpreted as representing an untreated tumor.

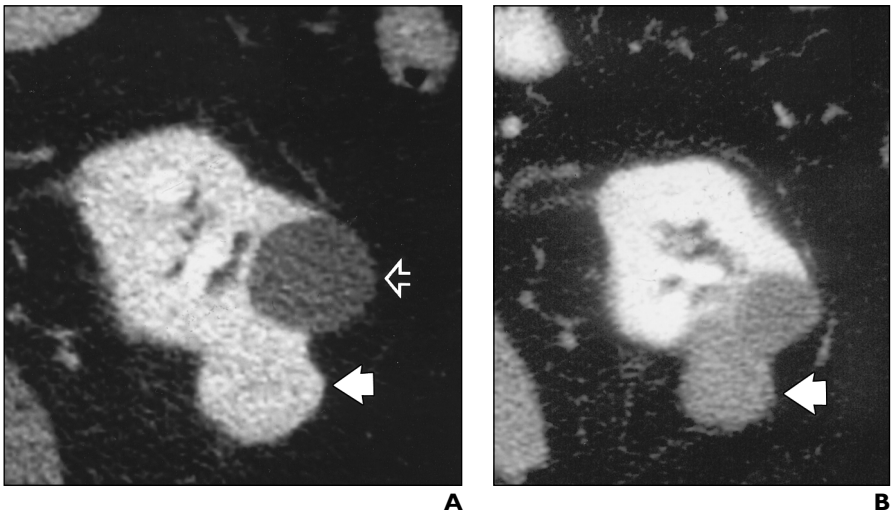

Fig. 5.—84-year-old man with 3.5-cm biopsy-proven renal cell carcinoma undergoing radiofrequency ablation.
A, Contrast-enhanced CT scan before therapy shows marked enhancement of solid exophytic tumor (*solid arrow*). Incidental simple cyst abuts tumor (*open arrow*).
B, Contrast-enhanced CT scan 6 months after ablation shows no contrast enhancement compared with baseline unenhanced study (*arrow*). Simple cyst is unchanged.

Fig. 6.—73-year-old woman with 6.5-cm metastasis from squamous cell carcinoma with inadequate treatment of tumor margins after radiofrequency (RF) ablation. CT image obtained 3 months after ablation shows enhancing bulky peripheral tumor growth (*arrows*) surrounding nonenhancing treated center (A). Five centimeters of coagulation was obtained with single 12-min RF application using clustered electrode approach.

Nuclear medicine has been used in a limited number of patients after ablation therapy. In one study, positron emission tomography scanning with a radioactive glucose analog (^{18}F-fluorodeoxyglucose) was used to detect active foci of residual tumor after percutaneous ethanol instillation in intrahepatic metastases [67].

Our current imaging strategy after thermal ablation includes an initial contrast-enhanced CT or MR study on the day of treatment to determine whether the patient has residual gross viable disease that requires immediate retreatment. Follow-up imaging is then performed at 1 and 3 months, and every 3–4 months thereafter. These scans are helpful in documenting the presence or absence of residual tumor that often may be amenable to additional thermal ablation treatment. If no evidence of peripheral tumor regrowth is seen by 6–12 months, adequate treatment can be inferred.

Trends for Thermal Ablation Therapy

The ultimate goal of tumor therapy is complete eradication of all malignant cells. Given the high likelihood of incomplete treatment by heat-based techniques alone, the case for combining thermal ablation with other therapies such as chemotherapy or chemoembolization cannot be overstated. A similar multidisciplinary approach including surgery, radiation, and chemotherapy is used for the treatment of most solid tumors. Given the variety of tumor types and organ sites to be treated, we think that it is overly optimistic to believe that all tumors can be destroyed with only one technique. Combination therapy is a key avenue of current ablation research.

Presently, many thermal ablation devices are being studied with multiple commercial devices now becoming available. Given the rapid pace of evolution in the state of the art for ablation technologies, we cannot confidently predict which method (if any) will prove dominant for any given clinical application. Competitive technologies must be able to ablate the desired volume of tissue in a reproducible and predictable fashion. However, other factors, including ease of clinical use and cost, will play a role in determining which of these technologies will receive the greatest attention.

Conclusion

Percutaneous imaging-guided thermal ablation therapy is an exciting and emerging arena that has thus far provided optimistic results for the minimally invasive treatment of selected focal neoplasms. Key questions that need to be addressed include definition of optimal methods and techniques for heating tumors, identification of optimal diagnostic imaging strategies to guide therapy and clinical follow-up, and determination of clinical impact for a given tumor or organ. For tumor heating, one must consider which technical innovations will enable efficient and efficacious energy deposition and which biologic factors can be successfully modulated to increase heat deposition and retention in the treated tumor. The answers to these questions will require substantial research that is ongoing at multiple tertiary centers. Hopefully, this work and well-conducted randomized multicenter trials will determine the proper role for this promising new paradigm of thermal ablation and the role these technologies will have throughout the general radiology community.

References

1. Goldberg SN, Livraghi T, Solbiati L, Gazelle GS. In situ ablation of focal hepatic neoplasms. In: Gazelle GS, Saini S, Mueller PR, eds. *Hepatobiliary and pancreatic radiology: imaging and intervention*. New York: Thieme, **1997**:470–502
2. De Sanctis JT, Goldberg SN, Mueller PR. Percutaneous treatment of hepatic neoplasms: a review of current techniques. *Cardiovasc Intervent Radiol* **1998**;21:273–296
3. Rossi S, Buscarini E, Garbagnati F, et al. Percutaneous treatment of small hepatic tumors by an expandable RF needle electrode. *AJR* **1998**;170: 1015–1022
4. Livraghi T, Goldberg SN, Meloni F, Solbiati L, Gazelle GS. Hepatocellular carcinoma: comparison of efficacy between percutaneous ethanol instillation and radiofrequency. *Radiology* **1999**; 210:655–663
5. Seki T, Wakabayashi M, Nakagawa T, et al. Ultrasonically guided percutaneous microwave coagulation therapy for small hepatocellular carcinoma. *Cancer* **1994**;74:817–825
6. Murakami R, Yoshimatsu S, Yamashita Y, Matsukawa T, Takahashi M, Sagara K. Treatment of hepatocellular carcinoma: value of percutaneous microwave coagulation. *AJR* **1995**;164:1159–1164
7. Solbiati L, Ierace T, Goldberg SN, et al. Percutaneous US-guided radio-frequency tissue ablation of liver metastases: treatment and follow-up in 16 patients. *Radiology* **1997**;202:195–203
8. Solbiati L, Goldberg SN, Ierace T, Livraghi T, Sironi S, Gazelle GS. Hepatic metastases: percutaneous radio-frequency ablation with cooled-tip electrodes. *Radiology* **1997**;205:367–374
9. Siperstein AE, Rogers SJ, Hansen PD, Gitomirsky A. Laparoscopic thermal ablation of hepatic neuroendocrine tumor metastases. *Surgery* **1997**; 122:1147–1155
10. Vogl TJ, Muller PK, Hammerstingl R, et al. Malignant liver tumors treated with MR imaging-guided laser-induced thermotherapy: technique and prospective results. *Radiology* **1995**;196: 257–265
11. Dodd GD, Halff GA, Rhim H, Chintapalli KN, Chopra S, Karahan OI. Radio-frequency thermal ablation of liver tumors (abstr). *Radiology* **1998**; 209(P):449
12. Anzai Y, Lufkin R, DeSalles A, Hamilton DR, Farahani K, Black KL. Preliminary experience with MR-guided thermal ablation of brain tumors. *AJNR* **1995**;16:39–48
13. McGovern FJ, Wood BJ, Goldberg SN, Mueller PR. Radiofrequency ablation of renal cell carcinoma via image guided needle electrodes. *J Urol* **1999**;161:599–600
14. Zlotta AR, Wildschutz T, Raviv G, et al. Radiofrequency interstitial tumor ablation (RITA) is a possible new modality for treatment of renal cancer: ex vivo and in vivo experience. *J Endourol* **1997**;11:251–258
15. Lewin JS, Connell CF, Duerk JL, et al. Interactive MRI-guided radiofrequency interstitial thermal ablation of abdominal tumors: clinical trial for evaluation of safety and feasibility. *J Magn Reson Imaging* **1998**;8:40–47
16. Rosenthal DI, Hornicek FJ, Wolfe MW, Jennings LC, Gephart MC, Mankin HJ. Changes in the management of osteoid osteoma. *J Bone Joint Surg Am* **1998**;80-A:815–821
17. Dupuy DE, Safran H, Mayo-Smith WW, Goldberg SN. Radiofrequency ablation of painful osseous metastases (abstr). *Radiology* **1998**;209 (P):389
18. Goldberg SN, Gazelle GS, Solbiati L, Rittman WJ, Mueller PR. Radiofrequency tissue ablation: increased lesion diameter with a perfusion electrode. *Acad Radiol* **1996**;3:636–644
19. Yeh MM, Trembly BS, Douple EB, et al. Theoretical and experimental analysis of air cooling for intracavitary microwave hyperthermia applicators. *IEEE Trans Biomed Eng* **1994**;41:874–882
20. Vogl TJ, Mack MG, Roggan A, et al. Internally cooled power laser for MR-guided interstitial laser-induced thermotherapy of liver lesions: initial clinical results. *Radiology* **1998**;209:381–385
21. Deardorff DL, Diederich CJ, Nau WH. Ultrasound applicators with internal cooling for interstitial thermal therapy. In: Ryan TP, Wong TZ, eds. *Thermal treatment of tissue with image guidance: proceedings*, vol. 3594. Bellingham, WA: Society of Photo-Optical Instrumentation Engineers, **1999**:36–46
22. Goldberg SN, Hahn PF, Tanabe KK, et al. Percutaneous radiofrequency tissue ablation: does perfusion-mediated tissue cooling limit coagulation necrosis? *J Vasc Interv Radiol* **1998**;9:101–111
23. Goldberg SN, Hahn PF, Halpern E, Fogle R, Gazelle GS. Radiofrequency tissue ablation: effect of pharmacologic modulation of blood flow on coagulation diameter. *Radiology* **1998**;209:761–769
24. Patterson EJ, Scudamore CH, Owen DA, Nagy AG, Buczkowski AK. Radiofrequency ablation of porcine liver in vivo: effects of blood flow and treatment time on lesion size. *Ann Surg* **1998;** 227:559–565
25. Heisterkamp J, van Hillegersberg R, Mulder PG, Sinofsky EL, Ijzermans JN. Importance of eliminating portal flow to produce large intrahepatic lesions with interstitial laser coagulation. *Br J Surg* **1997**;84:1245–1248
26. Pennes HH. Analysis of tissue and arterial blood temperatures in the resting human forearm. *J Appl Physiol* **1948**;1:93–122
27. Seegenschmiedt MH, Brady LW, Sauer R. Interstitial thermoradiotherapy: review on technical and clinical aspects. *Am J Clin Oncol* **1990**;13:352–363

28. Overgaard J. Hyperthermia as an adjuvant to radiotherapy: review of the randomized multicenter studies of the European Society for Hyperthermic Oncology. *Strahlenther Onkol* **1987**;163:453–457
29. Larson TR, Bostwick DG, Corica A. Temperature-correlated histopathologic changes following microwave thermoablation of obstructive tissue in patients with benign prostatic hyperplasia. *Urology* **1996**;47:463–469
30. Goldberg SN, Gazelle GS, Halpern EF, Rittman WJ, Mueller PR, Rosenthal DI. Radiofrequency tissue ablation: importance of local temperature along the electrode tip exposure in determining lesion shape and size. *Acad Radiol* **1996**;3:212–218
31. Goldberg SN, Solbiati L, Gazelle GS, Tanabe KK, Compton CC, Mueller PR. Treatment of intrahepatic malignancy with radio-frequency ablation: radiologic–pathologic correlation in 16 patients (abstr). *AJR* **1997**;168[American Roentgen Ray Society 97th Annual Meeting Program Book suppl]:121
32. Thomsen S. Pathologic analysis of photothermal and photomechanical effects of laser-tissue interactions. *Photochem Photobiol* **1991**;53:825–835
33. Cosman ER, Nashold BS, Ovelman-Levitt J. Theoretical aspects of radiofrequency lesions in the dorsal root entry zone. *Neurosurgery* **1984**;15: 945–950
34. Trembley BS, Ryan TP, Strohbehn JW. Interstitial hyperthermia: physics, biology and clinical aspects. In: Urano M, Douple E, eds. *Physics of microwave hyperthermia in hyperthermia and oncology*, vol 3. Utrecht, the Netherlands: Verlag Springer, **1992**:11–98
35. Amin Z, Brown SG, Lees WR. Liver tumor ablation by interstitial laser photocoagulation: review of experimental and clinical studies. *Semin Intervent Radiol* **1993**;10:88–100
36. Cline HE, Hynynen K, Watkins RD, et al. Focused US system for MR imaging-guided tumor ablation. *Radiology* **1995**;194:3:731–737
37. Diederich CJ, Nau WH, Deardorff DL, et al. Prostate thermal therapy with interstitial and transurethral ultrasound applicators: a feasibility study. In: Ryan TP, ed. *Surgical applications of energy: proceedings*, vol. 3294. Bellingham, WA: Society of Photo-Optical Instrumentation Engineers, **1998**:2–13
38. Honda N, Guo Q, Uchida H, Ohishi H, Hiasa Y. Percutaneous hot saline injection therapy for hepatic tumors: an alternative to percutaneous ethanol injection therapy. *Radiology* **1994**;190:53–57
39. McGahan JP, Brock JN, Tessluk H, Gu WZ, Schneider P, Browning PD. Hepatic ablation with use of radio-frequency electrocautery in the animal model. *J Vasc Interv Radiol* **1992**;3:291–297
40. Goldberg SN, Gazelle GS, Dawson SL, Rittman WJ, Mueller PR, Rosenthal DI. Tissue ablation with radiofrequency: effect of probe size, gauge, duration, and temperature on lesion volume. *Acad Radiol* **1995**;2:399–404
41. Nolsoe CP, Torp-Pedersen S, Burcharth F, et al. Interstitial hyperthermia of colorectal liver metastases with a US-guided ND-YAG laser with a diffuser tip: a pilot clinical study. *Radiology* **1993**; 187:333–337
42. Goldberg SN, Gazelle GS, Dawson SL, Mueller PR, Rittman WJ, Rosenthal DI. Radiofrequency tissue ablation using multiprobe arrays: greater tissue destruction than multiple probes operating alone. *Acad Radiol* **1995**;2:670–674
43. Amin Z, Donald JJ, Masters A, et al. Hepatic metastases: interstitial laser photocoagulation with real-time US monitoring and dynamic CT evaluation of treatment. *Radiology* **1993**;187:339–347
44. Leveen RF. Laser hyperthermia and radiofrequency ablation of hepatic lesions. *Semin Intervent Radiol* **1997**;14:313–324
45. Goldberg SN, Gazelle GS, Solbiati L, Mullin K, Rittman WJ, Mueller PR. Large volume radiofrequency tissue ablation: increased coagulation with pulsed technique (abstr). *Radiology* **1997**; 205(P):258
46. Nishioka NS, Domankevitz Y, Flotte TJ, Anderson RR. Ablation of rabbit liver, stomach and colon with a pulsed holmium laser. *Gastroenterology* **1989**;96:831–837
47. Goldberg SN, Stein M, Gazelle GS, Kruskal J, Clouse ME. Percutaneous RF tissue ablation: optimization of pulsed-radio-frequency technique to increase coagulation necrosis. *J Vasc Interv Radiol* **1999**;10:907–916
48. Livraghi T, Goldberg SN, Monti F, et al. Saline-enhanced radio-frequency tissue ablation in the treatment of liver metastases. *Radiology* **1997**; 202:205–210
49. Hoey MF, Paul S, Nakib NA. Saline spread and conductivity of the liquid electrode in the liver for radiofrequency energy application (abstr). *Radiology* **1998**;209(P):448
50. Merkle E, Goldberg SN, Lewin JS. Effect of superparamagnetic MR contrast agents on radiofrequency ablation. *Radiology* **1999**;212:459–466
51. Dupuy DE, Goldberg SN, Gazelle GS, Rosenthal DI. Cooled-tip radio-frequency ablation in the vertebral body: temperature distribution in the spinal canal (abstr). *Radiology* **1997**; 807(P):330
52. Murakami T, Shibata T, Ishida T, et al. Percutaneous microwave hepatic tumor coagulation with segmental hepatic blood flow occlusion in seven patients. *AJR* **1999**;172:637–640
53. Goldberg SN, Gazelle GS, Solbiati L, et al. Percutaneous radiofrequency liver tumor ablation. *AJR* **1998**;170:1023–1028
54. Malone DE, Lesiuk L, Brady AP, Wyman DR, Wilson BC. Hepatic interstitial laser photocoagulation: demonstration and possible clinical importance of intravascular gas. *Radiology* **1994**; 193:233–237
55. Goldberg SN, Walovitch R, Halpern EF, Gazelle GS. Immediate detection of radiofrequency induced coagulation necrosis using an ultrasound contrast agent. *Radiology* **1999;**213:438–444
56. Bartolozzi C, Lencioni R, Ricci P, Paolicchi A, Rossi P, Passariello R. Hepatocellular carcinoma treatment with percutaneous ethanol injection: evaluation with contrast-enhanced color Doppler US. *Radiology* **1998**;209:387–393
57. Hyodoh H, Hyodoh K, Takahashi K, et al. Microwave coagulation therapy on hepatomas: CT and MR appearance after therapy. *J Magn Reson Imaging* **1998**;8:451–458
58. Mitsuzaki K, Yamashita Y, Nishiharu T, et al. CT appearance of hepatic tumors after microwave coagulation therapy. *AJR* **1998**;171:1397–1403
59. Boaz TL, Lewin JS, Chung YC, Duerk JL. MR monitoring of MR-guided radiofrequency thermal ablation of normal liver in an animal model. *J Magn Reson Imaging* **1998**;8:64–69
60. Mueller-Lisse UG, Thoma M, Faber S, et al. Coagulative interstitial laser-induced thermotherapy of benign prostatic hyperplasia: online imaging with a T2-weighted fast spin-echo MR sequence–experience in six patients. *Radiology* **1999**;210: 373–379
61. Steiner P, Botnar R, Goldberg SN, Gazelle GS, Debatin JF. Monitoring of radio-frequency tissue ablation in an interventional MR environment: preliminary ex vivo and in vivo results. *Invest Radiol* **1997**;32:671–678
62. Busse H, Rassek M, Grust A, Kahn T, Schwarzmaier HJ. Improved qualitative MR thermometry using a 1.5 T scanner to monitor cooled applicator systems during laser-induced interstitial thermotherapy (LITT). In: Ryan TP, Wong TZ, eds. *Thermal treatment of tissue with image guidance*: *proceedings*, vol. 3594. Bellingham, WA: Society of Photo-Optical Instrumentation Engineers, **1999**:96–203
63. Samulski TV, Jones E, Henke F, Buffalo C, Scott T, MacFall JM. Magnetic resonance image guided thermal therapy with a radiofrequency phased array. In: Ryan TP, Wong TZ, eds. *Thermal treatment of tissue with image guidance*: *proceedings*, vol. 3594. Bellingham, WA: Society of Photo-Optical Instumentation Engineers, **1999**:124–128
64. Zhang, Q, Chung, YC, Lewin, JS, Duerk, JL. A method for simultaneous radiofrequency ablation and MRI. *J Magn Reson Imaging* **1998**;8:110–114
65. Solbiati L, Goldberg SN, Ierace T, DellaNoce M, Livraghi T, Gazelle GS. Microbubble ultrasound contrast agents: a useful adjunct for radiofrequency tumor ablation. *Radiology* **1999**;211:643–649
66. Goldberg SN, Mallery S, Brugge W, Gazelle GS. Endoscopic ultrasound: guided radiofrequency (RF) ablation in pancreas—results in porcine model. *Gastrointest Endosc* **1999**;50:392–401
67. Dawson SL, Mueller PR, Lee MJ, Boland GW, Goldberg MA, Fischman AJ. Value of PET imaging in evaluation of percutaneous ablation of malignant hepatic neoplasms (abstr). *Radiology* **1994**;193(P)582:221

APPENDIX: Bioheat Equation as Outlined by Pennes [26]

The bioheat equation takes into account the factors that influence tissue heating and states:

$$\rho_t c_t \partial T(r,t) / \partial t = \nabla (k_t \nabla T) - c_b \rho_b m \rho_t (T - T_b) + Q_p (r,t) + Q_m (r,t)$$

where:

- ρ = density of tissue, blood (kg/m^3)
- c = specific heat of tissue, blood (W sec/kg °C)
- k = thermal conductivity
- m = perfusion (blood flow rate / unit mass tissue) (m^3/kg sec)
- Qp = power absorbed / unit volume tissue
- Qm = metabolic heating / unit volume of tissue

This formula takes into account the variables that influence tissue heating and thus can help explain and predict the extent of ablation produced by thermal energy under a variety of circumstances. This equation can be simplified to a first approximation as:

Coagulation necrosis = energy deposited × local tissue interactions – heat lost.